Analytical Investigation of Induction Motor Drive under DC-Link Voltage Ripple in Voltage Source Inverter

J. Klima[1]

[1]Department of Electrical Engineering and Automation, Technical Faculty of CZU, 165 21 Prague 6 -Suchdol, Czech Republic, e-mail: klima@tf.czu.cz

Abstract. Analytical analysis and mathematical model of ripple components of the DC-link voltage of three-phase voltage source inverter and its influence on an induction motor drive both in time and frequency domain are presented in this paper. The analytical expressions for the voltage and current space-vectors as a function of the DC-link voltage pulsation are derived. From the current space vectors the torque behavior is estimated again as a function of DC-link voltage pulsation. The proposed analytical method is based on the mixed p-z approach enabling presentation of the results in closed-form.

Key words

DC-Link Voltage Ripple, Induction Motor Drive, Electromagnetic Torque, VSI

1. Introduction

The use of the voltage source inverters (VSI) with DC-links for feeding of induction motor drives is getting more and more common. In general DC-link voltage spectrum consists of the DC components responsible for power delivery, plus ripple components.
The inverter experiences in some situations a substantial ripple of DC-link voltage may negatively affect the supply of connected electric drives.
The DC-link voltage pulsation is composed of several sources such as [1] [2], [3].
a) The diode rectification of the AC line voltage causes pulsation components
b) Unbalance in the AC power supply generates 100 or 120-Hz component
c) In some faulty conditions in the front-end rectifier DC-link voltage may consist again pulsation
An increase in electric losses, excessive rise of the motor temperature, appearance of the torque pulsation, and noise problems are just some of the possible problems.
So, the analysis of the DC-link pulsation and its influence on the motor performances is of great importance.
In this paper, analytical model and analysis of the DC-link pulsation is presented. The analytical closed-form expressions for the stator and rotor currents are derived. From these equations an analytical expression for the electromagnetic torque in dependence of DC-link pulsation is derived.
The mathematical model is based on the mixed p-z approach [9] enabling solution in closed-form .The analytical derived results are visualized by the programme MATCAD [11].

2. Mathematical model

From Fig.1 we can see the basic diagram for VSI fed induction motor drive with DC-link voltage Vdc
For the mathematical model we assume that the capacitor DC-link voltage can be expressed with the constant value V_{dc} and pulsation part $\Delta V_{dc}.\cos\omega t$
As shown in [2] voltage ripple with an angular frequency $\omega = 2.\omega_0$,where ω_0 is an angular frequency of the supply voltage (314 rad/sec) may be caused by unbalance of three-phase voltage supply of the PWM rectifier (the front-end stage of the converter).
In that case we can express the voltage space-vector of the motor can be expressed in n-th sector as follows:

$$\left[V_{dc}+\Delta V_{dc}\cos\left[2.\omega_0.(n+\varepsilon).T\right]\right].e^{j.n.\frac{\pi}{3}} = V_0(n,\varepsilon)+V_1(n,\varepsilon) \tag{1}$$

where two parts in (1) are given as follows:
The voltage space vector from the constant DC-link voltage

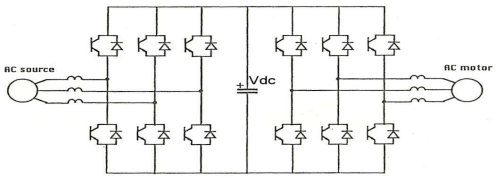

Fig.1. Basic scheme of VSI with AC motor

$$V_0(n,\varepsilon) = \frac{2}{3}V_{dc}.e^{j.n.\frac{\pi}{3}} \tag{2}$$

The voltage space vector from the pulsation of the DC-link voltage

$$V_1(n,\varepsilon)=\frac{2}{3}\Delta V_{dc}e^{j.n.\frac{\pi}{3}}.\cos(2.\omega_0.(n+\varepsilon).T)=\frac{1}{3}\Delta V_{dc}e^{j.n.\frac{\pi}{3}}.e^{j.2.\omega_0.(n+\varepsilon).T}+$$

$$\frac{1}{3}\Delta V_{dc}e^{j.n.\frac{\pi}{3}}.e^{-j.2.\omega_0.(n+\varepsilon).T}=V_{1P}(n,\varepsilon)+V_{1N}(n,\varepsilon) \tag{3}$$

In (1) time is expressed in per unit as follows:

$$t=(n+\varepsilon)T=(n+\varepsilon)T_1/6\ ,$$

where n is number of a sector, T= $T_1/6$ is a sector interval, ε is a per unit time inside of a sector $0 \le \varepsilon \le 1$ and T_1 is a fundamental output frequency.
As can be seen from (3) the part that includes DC-link pulsation can be separated into two additional parts, namely positive and negative ones.
The trajectory of the stator voltage space vector given by (3) is shown in Fig.2.The trajectory of the constant DC-link voltage part given by (2) is shown in Fig. 3.The overall trajectory is composed of the two parts: $V_0(n, \varepsilon)$ is the constant part and $V_1(n, \varepsilon)$ the pulsation part. The overall trajectory of the stator voltage vector given by (1) is shown in Fig.4.
Fig.5 shows the waveform of the pulsation part of the voltage space vector (real part), given by

$$V_{1real}(n,\varepsilon)) = \mathrm{Re}(V_1(n,\varepsilon)) = \mathrm{Re}(V_{1P}(n,\varepsilon) + V_{1N}(n,\varepsilon)) \quad (4)$$

The steady-state voltage waveforms (real parts) of the negative and positive parts of (4) are shown in Fig.6

Fig.2 Trajectory of DC-link pulsation part of stator voltage vector, $f_0=f_1$, $\Delta V_{dc} = 0.1$

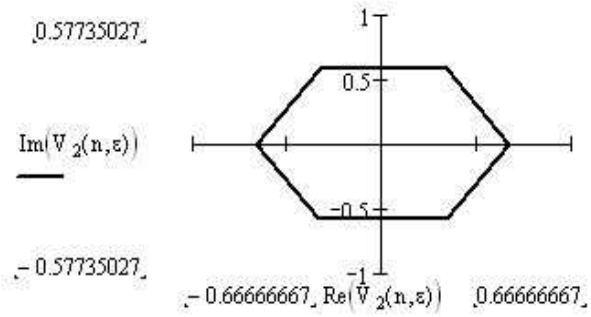

Fig.3 Trajectory of DC-link constant part of stator voltage vector

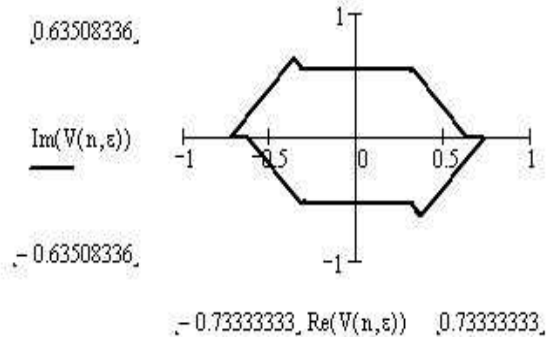

Fig.4-Trajectory of overall stator voltage vector

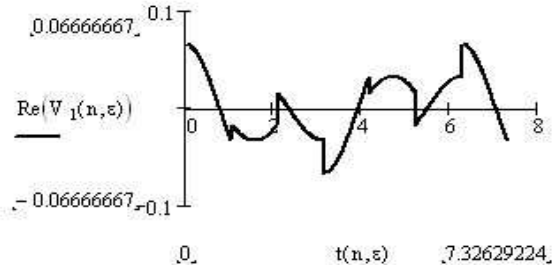

Fig.5.Voltage waveform of real part of pulsation space vector

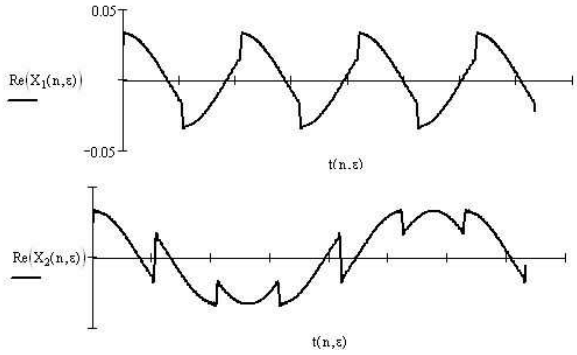

Fig.6 Voltage waveforms of positive (top) and negative (bottom) parts of DC-link pulsation

3. Time-domain analysis

Using mixed p-z approach as shown in [9] we can erive in the closed-form analytical expressions for the stator and rotor currents and also for the electromagnetic torque. From these relations we can estimate the influence of the DC-link voltage pulsation of the currents and/or electromagnetic torque.
The solution for the stator currents can be expressed in closed-form as follows:

$$I_S(n,\varepsilon) = I_{SC}(n,\varepsilon) + I_{SP}(n,\varepsilon) + I_{SN}(n,\varepsilon) \quad (5)$$

Similarly we can express solution for the rotor currents:

$$I_R(n,\varepsilon) = I_{RC}(n,\varepsilon) + I_{RP}(n,\varepsilon) + I_{RN}(n,\varepsilon) \quad (6)$$

where $I_{SC}(n,\varepsilon)$, $I_{RC}(n,\varepsilon)$, are the stator, rotor current components from the constant part of the DC-link voltage, $I_{SP}(n,\varepsilon)$, $I_{RC}(n,\varepsilon)$ are the stator, rotor current components from the positive part of the ripple DC-link voltage, $I_{SN}(n,\varepsilon)$, $I_{RN}(n,\varepsilon)$ are the stator, rotor current components from the negative part of the ripple DC-link voltage
Some of these results are shown in Figs7-10

The analytical results are given for the following motor parameters (in per units):

$R_S=R_R=0.02, L_S=L_R=3.0$, $L_m=2.9$, slip s=0.02,
$V_{dc}=1.0$, $\Delta V_{dc}=0.1$, $f_0=f_1=50$ Hz.

From Fig.7 we can see the trajectory of the steady-state stator current vectors $I_{SP}(n,\varepsilon)+I_{SN}(n,\varepsilon)$ and from Fig.8 we can see two parts forming the overall pulsating trajectory. The trajectory given by the positive part of+ DC-link ripple voltage (top trace) and part from the negative DC-link ripple voltage (bottom trace).
The phase waveforms of these trajectories are given in Fig.9.We can see the overall phase current (doted), the phase current from the constant DC-link voltage (dashed) and difference which is caused by the pulsation of the DC-link voltage (full black line).
The phase current waveforms of the negative and positive currents components are shown in Fig.10

From Fig.11 we can see the overall electromagnetic torque having bigger pulsation part owing to the DC-link pulsation.
The electromagnetic torque can be determined again in closed-form as follows:

$$T_i(n,\varepsilon)=\frac{3}{2}p_p L_m \operatorname{Re}\left\{jI^{*}_{S}(n,\varepsilon)I_R(n,\varepsilon)\right\} \qquad (7)$$

Where * means complex conjugate value

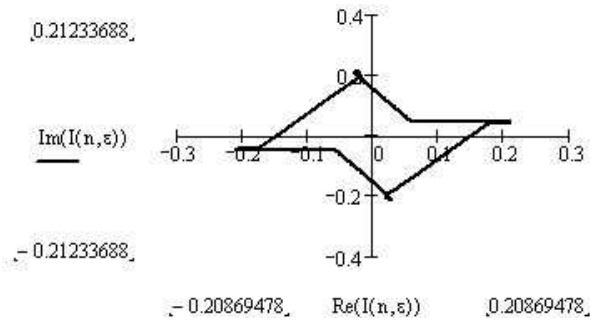

Fig.7 Overall stator current trajectory in complex plane

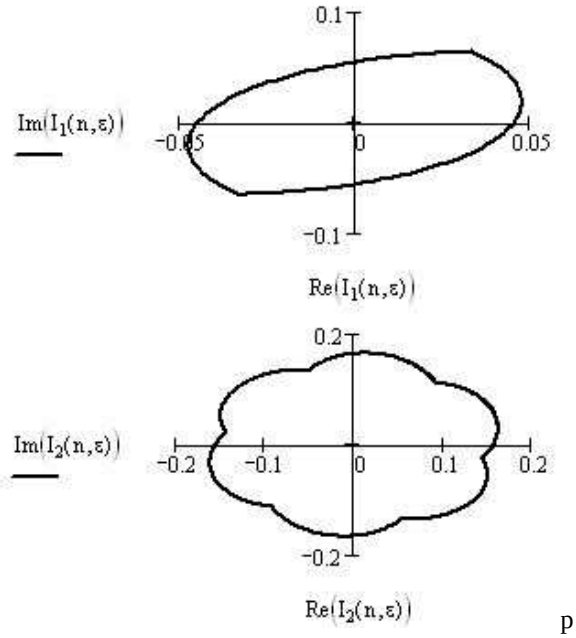

p

Fig.8.Two components forming the overall stator current trajectory

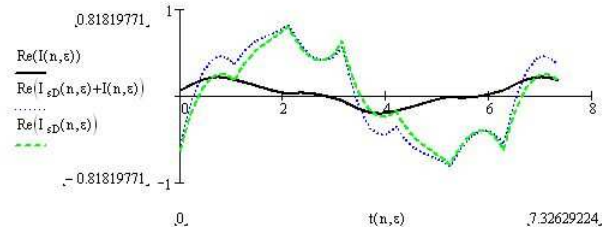

Fig.9 Phase current waveforms respecting the DC-link voltage ripple

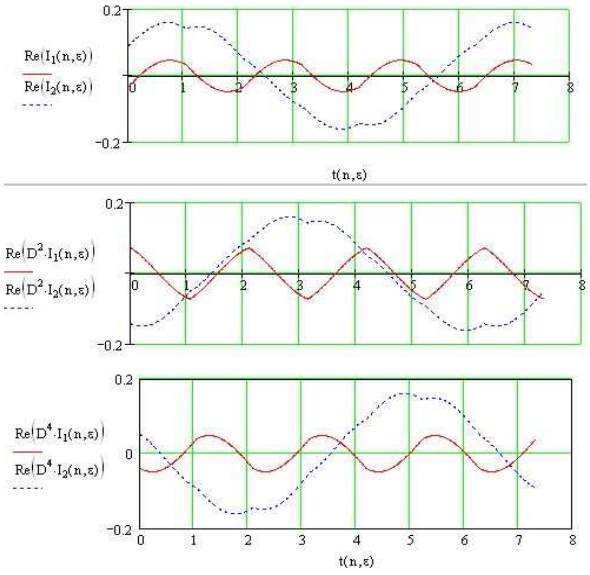

Fig.10 Phase currents waveforms. Positive part (dotted).Negative part (solid)

Fig 12 shows the electromagnetic torque from DC-link constant voltage (top trace) and the difference from the overall and constant voltage waveform (part forming the additional torque pulsation)

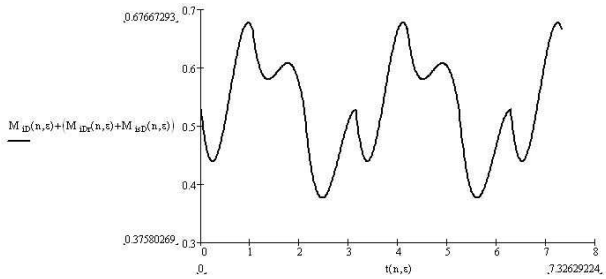

Fig.11 Electromagnetic overall torque waveform.

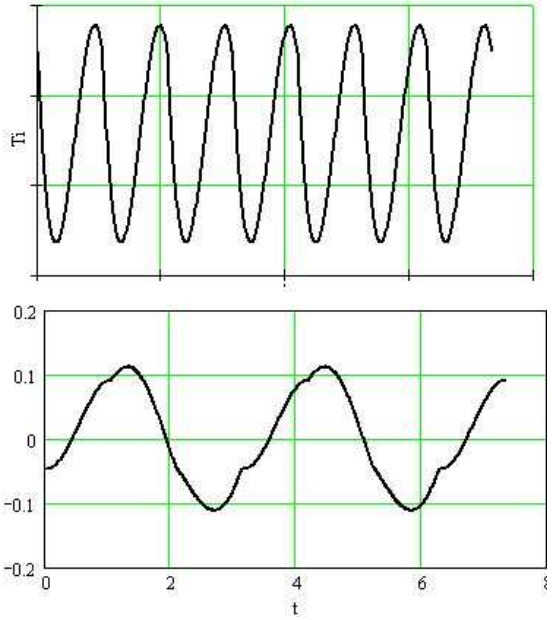

Fig.12. Electromagnetic torque waveforms. Top – without any DC link components. Bottom -Contribution from DC link ripple.

The situation is for the sake of clarity shown once more in Fig.13.Part forming the additional torque component is again shown in Fig.13 (green line).This additional torque is composed of the two parts. First one (black line) is given by the constant stator currents and ripple rotor components; second one (red line) is given by the constant rotor currents and ripple stator components. As can be seen from Fig.13 both components with high values are acting with nearly opposite direction and forming the overall pulsation waveform.

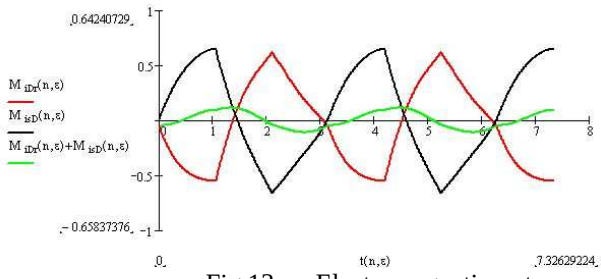

Fig.13. Electromagnetic torques. Contribution of DC link ripples (green) and its two parts (black and red lines).

4. Frequency-domain analysis

The Fourier series of the voltage space vector without DC-link ripple components $U(n,\varepsilon)$ can be expressed as:

$$U(n,\varepsilon) := \sum_{\nu=-20}^{20} C(\nu)\cdot e^{j\cdot(n+\varepsilon)\cdot T\cdot\omega_1\cdot(1+6\cdot\nu)}$$

$$X_1(n,\varepsilon) := \frac{U(n,\varepsilon)}{2}\cdot e^{j\cdot[2\cdot\omega_0\cdot(n+\varepsilon)\cdot T]}$$

$$X_2(n,\varepsilon) := \frac{U(n,\varepsilon)}{2}\cdot e^{-j\cdot[2\cdot\omega_0\cdot(n+\varepsilon)\cdot T]} \qquad (8)$$

The Fourier coefficients in (8) are given by

$$C(\nu) := \frac{\Delta V_{dc}\cdot 2}{\pi j\cdot(1+6\cdot\nu)} \qquad (9)$$

And the overall trajectory can be expressed as follows:

$$X(n,\varepsilon) = X_1(n,\varepsilon) + X_2(n,\varepsilon) \qquad (10)$$

$X_1(n,\varepsilon)$ and $X_2(n,\varepsilon)$ includes the positive and negative part of the DC-link ripple voltage.The voltage harmonic spectrum is shown in Fig.14

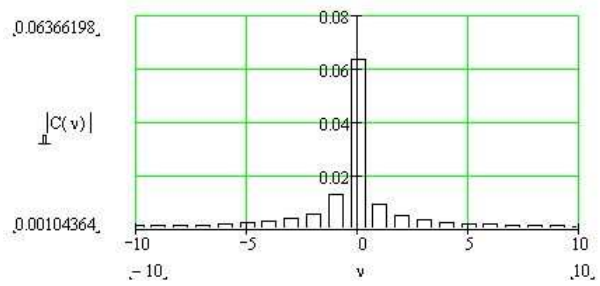

Fig.14.Voltage harmonic spectrum

Owing to additional side harmonics the voltage spectrum contains harmonics order of (1+6ν) f_1 $\pm 2\, f_0$.For example if $f_0=f_1=50$ Hz, the harmonic spectrum contains orders of

6ν+3 (in $X_1(n,\varepsilon,\nu)$) and 6ν-1 (in $X_2(n,\varepsilon,\nu)$), where $\nu = 0,\pm1,\pm2....$

Fig.15 shows time dependency of the first three harmonics of $X_1(n,\varepsilon,\nu)$ for $\nu=0, \nu=\pm1$

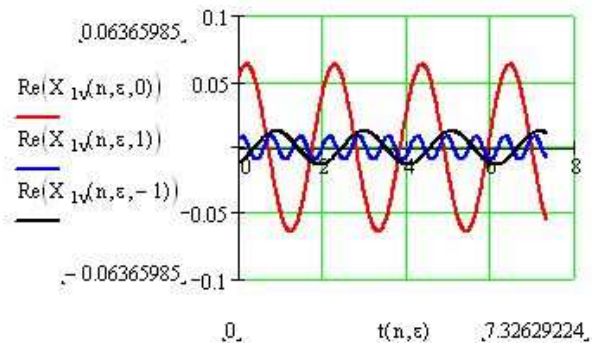

Fig.15.Voltage harmonic waveforms for ν=0 (red line), ν=1 (blue line), ν=-1, (black line)

From Fig.16 we can see the Fourier approximation of the of DC-link pulsation part of stator voltage vector. This waveform can be compared with Fig.2 where is analytical trajectory of the same dependency. Comparing both figures we can see very good approximation validating frequency-domain analysis.

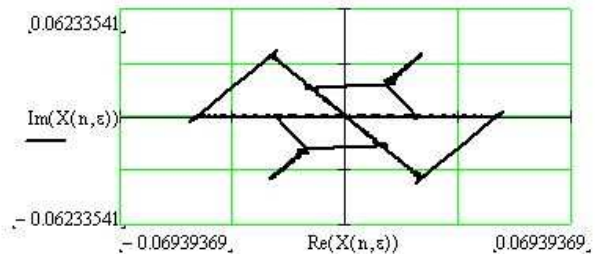

Fig.16.Fourier approximation of the of DC-link pulsation part of stator voltage vector

Fig.17 shows the Fourier approximation of the two parts X_1 (n,ε) and X_2 (n,ε) forming the overall trajectory $X(n,\varepsilon) = X_1(n,\varepsilon) + X_2(n,\varepsilon)$

4. Conclusion

Analytical analysis and mathematical model of three-phase voltage source inverter fed induction motor drive under DC-link voltage pulsation are presented in this paper. The analytical expressions for the voltage and current space-vectors as a function of the DC-link voltage pulsation are derived. By means of the modified Z-transform and the mixed p-z mathematical model we can estimate the separate parts of the solution to judge the influence of the DC-link voltage pulsating

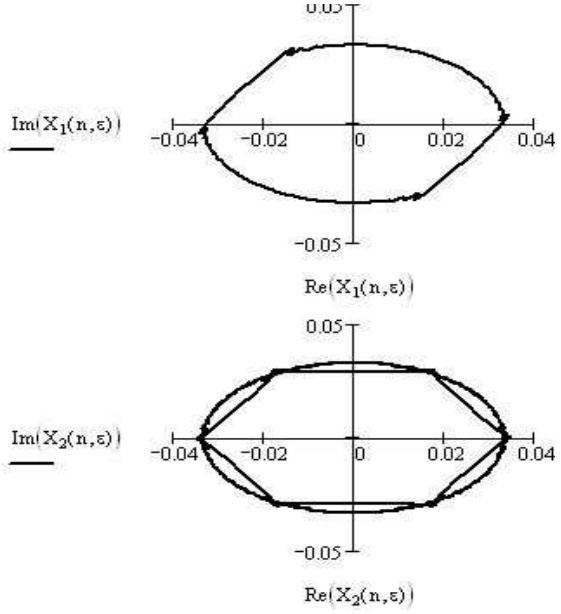

Fig.17. Fourier approximation2 of $X_1(n,\varepsilon)$ (top) an $X_2(n,\varepsilon)$ (bottom)

REFERENCES:

[1]. CROSS,A,M.,EVANS,P.D.,FORSYTH,A.J.: DC link current in PWM inverters with unbalanced and non-linear loads.IEE Proc.Electr.Pow.Appl.Vo.143,No,6.1999,pp.620-626

[2]. CHOMAT,M.,SCHREIER,L.:Mathematical and numerical modeling of controlled rectifier under unbalanced three-phase voltage supply. IEMDC Conference,Madison,USA,2003,pp.452-459

[3]. BROECK H.W.,SKUDELNY H.C.: Analytical Analysis of the Harmonic Effects of a PWM AC Drive.IEEE Trans.Power Electron.1988,(2),pp.216-222.

[4]. BROECK H.W.,WYK J.D..:A Comparative Investigation of a Three-Phase Induction Machine Drive with a Component Minimised Voltage-Fed Inverter under Different Control Options.IEEE Trans.Ind.Appl.1984,(2),pp.309-320.

[5]. BLAABJERG F.,FREYSSON S.,HANSEN H.,HANSEN S.: A New Optimised Space-Vector Modulation Strategy for a Component-Minimized Voltage Source Inverter.IEEE Trans.Power Electron.(1997),(4),pp.704-713.

[6] C.CECEATI, N.ROTONDALE. : A double PWM-strategy for improved electric drive reliability. Proceedings of Conf.Speedam, 2002, pp.A2-25-A2-30.

[7]. KLIMA J.: Using of Discrete Fourier Transform for the Analysis of the Circuits with the Periodical Modulation. Journal of Electrical Eng.(1988),(4),pp.257-265.

[8] . KLIMA J.: Analytical Closed-Form Solution of a Space-Vector Modulated VSI Feeding an Induction Motor Drive.IEEE Transaction on Energy Conversion.Vol.17,No2.June2002,pp.191-196.